Journal of Alloys and Compounds 509 (2011) 9558–9561

Contents lists available at ScienceDirect

Journal of Alloys and Compounds

journal homepage: www.elsevier.com/locate/jallcom

Deformation and microstructure evolution of a high strain rate superplastic Mg–Li–Zn alloy

Xuhe Liu*, Guanjun Du, Ruizhi Wu*, Zhongyi Niu, Milin Zhang

Key Laboratory of Superlight Materials & Surface Technology (Harbin Engineering University), Ministry of Education, Harbin 150001, PR China

ARTICLE INFO

Article history:
Received 10 May 2011
Accepted 24 July 2011
Available online 29 July 2011

Keywords:
Mg–Li alloy
High strain rate superplasticity
Deformation mechanism
Microstructure evolution

ABSTRACT

An Mg–8Li–2Zn alloy plate was prepared through a two-pass extrusion process, and the high-temperature behavior of the alloy was investigated at 473–593 K under the initial strain rate of 1.0×10^{-2}–1.0×10^{-1} s^{-1}. The results indicated that the alloy exhibits a significant high strain rate superplasticity with a maximum elongation of 279% under an initial strain rate of 1.0×10^{-2} s^{-1}. The activation energy is 89.4 kJ/mol, indicating that the dominant deformation mechanism in the alloy is grain-boundary sliding controlled by grain-boundary diffusion. Cavities nucleate and coalesce during deformation, which is one of the results leading to the fracture of the material.

1. Introduction

There is a considerable interest in the application of wrought Mg–Li alloys in the aerospace and 3C industry due to their good properties [1–3]. The formability of Mg–Li alloys has been proved to improve significantly in the superplastic state, accordingly, the Mg–Li alloys can be used effectively in the fabrication of airframes, thin-walled and stiffened panels where high workability is required [4].

Previous works have indicated that superplaticity occurs in Mg–Li alloys at elevated temperature or under low strain rate [5,6], including the cast Mg–Li alloy [7], the conventional extruded Mg–Li alloy [8], rolled Mg–Li alloy [9], ECAP Mg–Li alloy [10] and Mg–Li based composites [11]. The development of superplasticity has two directions, low-temperature superplasticity and high strain rate superplasticity. As for Mg–Li alloy, the high strain rate superplasticity has more practical significance due to the high production efficiency. Although the high strain rate superplasticity generally corresponds to the high temperature, the temperature is usually in the range of 573–673 K for Mg–Li alloy which belongs to the low level in the industry. Therefore, under this temperature range, the superplasticity process is easy to be implemented without ignition or much oxidation. However, only few of them were founded to show large elongation at high strain rate more than 10^{-2} s^{-1} [12]. Therefore, similar to Al alloys [13–15] and other metal-based materials, high strain rate superplasticity in Mg–Li alloys would be beneficial to their commercial forming applications.

In this paper, an Mg–8Li–2Zn alloy was prepared through a processing of two-pass extrusion and the superplastic characteristics and microstructure evolution under the high strain rate of the alloy was investigated.

2. Experimental

Pure magnesium, pure lithium, and pure zinc were used to prepare the ingots in a vacuum induction furnace under argon shield, and the melt was poured into a 106 mm diameter permanent mould in the furnace to obtain Mg–Li–Zn alloy ingot. The ingot was heat-treated at 573 K for 24 h and then extruded for two-pass at 553 K to obtain a plate with a width of 30 mm and a thickness of 3 mm.

Tensile specimens were machined parallel to the extrusion direction with a gauge length of 10 mm and a gauge width of 6 mm. The tensile tests were conducted at elevated temperature using a WDW3050 testing machine with a constant speed of the cross-head displacement, and the temperature accuracy was controlled within ±2 K. Tests were conducted at initial strain rates of 1.0×10^{-2}–1.0×10^{-1} s^{-1} and temperatures of 473–623 K.

The microstructures of specimens before and after tensile testing were measured with optical microscope (OM). The specimens were etched with a 2 vol.% nital.

3. Results and discussion

3.1. Microstructure of the extruded alloys

The microstructures of the alloy are shown in Fig. 1. The alloy is composed of 62% β-Li phase (black part) and 38% α-Mg phase (white part). The α-Mg phase distributes along the extrusion direction. The grain size of α-Mg phase and β-Li phase are all less than

* Corresponding authors at: College of Materials Science & Chemical Engineering, Harbin Engineering University, 145 Nantong St., Harbin 150001, PR China. Tel.: +86 451 82519696; fax: +86 451 82519696.
E-mail addresses: liuxuhe@gmail.com (X. Liu), Ruizhiwu2006@yahoo.com (R. Wu).

0925-8388/$ – see front matter © 2011 Elsevier B.V. All rights reserved.
doi:10.1016/j.jallcom.2011.07.081

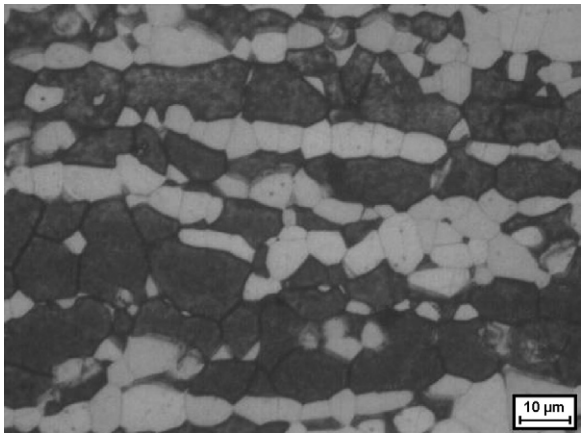

Fig. 1. Microstructures of the extruded specimen.

Table 1
Tensile elongation of the alloy under different tensile parameters.

Initial strain rate, s^{-1}	Temperature, K	Tensile elongation, %
1×10^{-2}	473	105
	523	148
	573	178
	623	279
5×10^{-2}	473	100
	523	115
	573	150
	623	173
1×10^{-1}	473	79
	523	107
	573	146
	623	151

10 μm, which is a qualified microstructure for the superplastic behavior.

3.2. Elevated-temperature tensile properties of the alloy

The elongation percentages of the alloy under different tensile parameters are listed in Table 1 and the stress–strain curves of the specimens are shown in Fig. 2. With the decrease of initial strain rate and the increase of temperature, the maximum strain of the alloy increases. The elongations to failure of the alloy are all higher than 100% except when under an initial strain rate of $1.0 \times 10^{-1}\ s^{-1}$ at 473 K, and the largest elongation of 279% can be obtained at the temperature of 623 K under the initial strain rate of $1.0 \times 10^{-2}\ s^{-1}$. Even when the initial strain rate is $1.0 \times 10^{-1}\ s^{-1}$, the maximum elongation is larger than 150%, indicating the alloy exhibits notable high strain rate superplasticity.

The flow stress decreases with the increase of test temperature and the decrease of strain rate. In addition, specimens tested at high temperature indicate a steady state flow region, and the lower initial strain rate is, a longer time the stable flow stress sustains. A long time of stable flow suggests that the progress of necking is extremely gradual in those specimens. It is thought that dynamic recovery or recrystallization occurs and deformation progresses with balancing of work hardening in the steady state flow region.

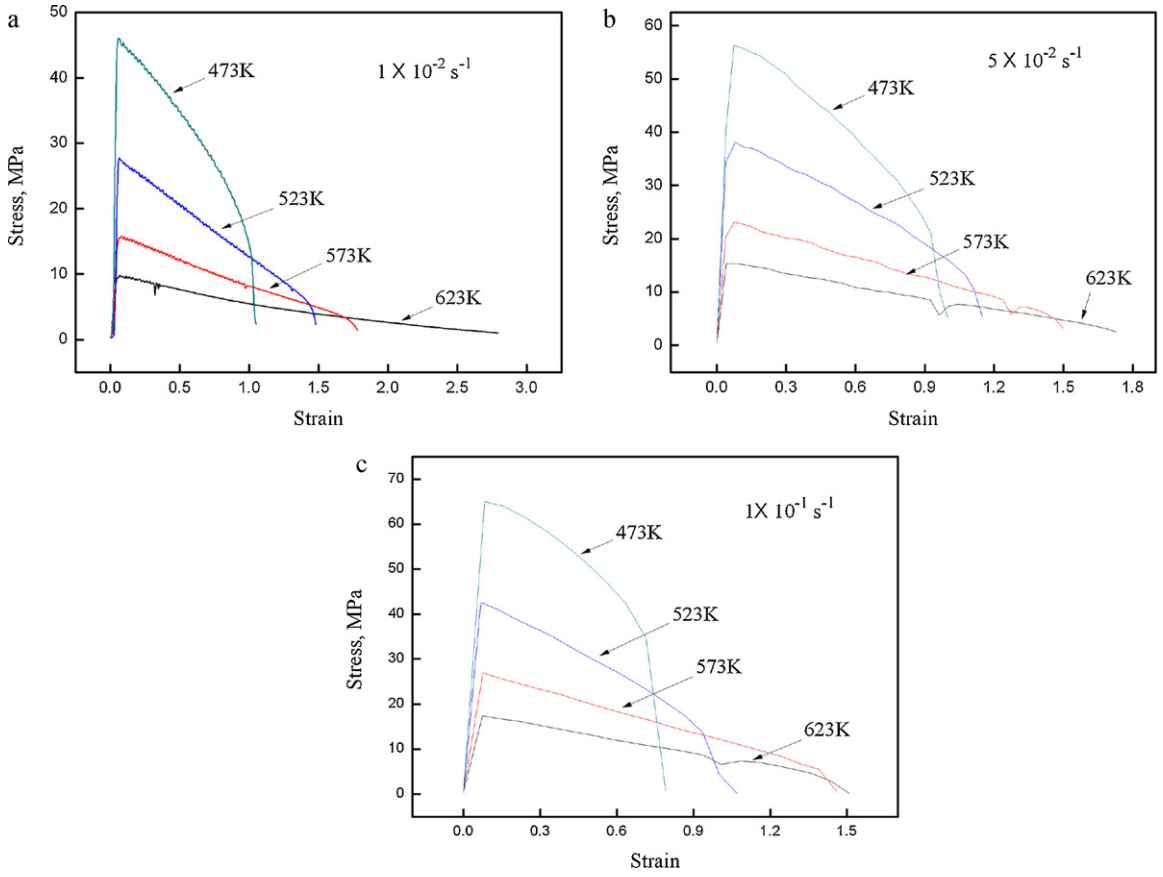

Fig. 2. The stress–strain curves during superplastic tension: (a)–(c) specimens at different temperatures with initial strain rate of $1 \times 10^{-2}\ s^{-1}$, $5 \times 10^{-2}\ s^{-1}$ and $1 \times 10^{-1}\ s^{-1}$.

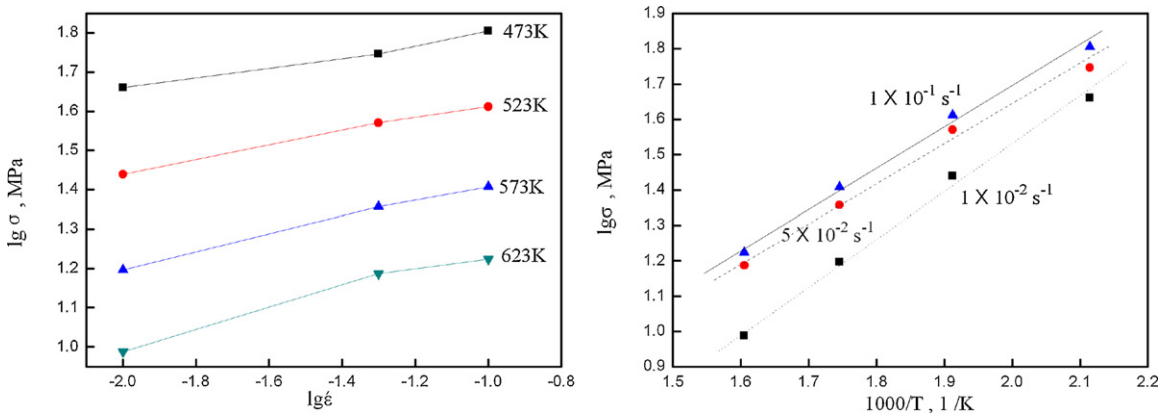

Fig. 3. The $\lg\sigma$ versus $\lg\dot{\varepsilon}$ curves and $\lg\sigma - 1/T$ curves of the two-pass alloy.

3.3. Deformation activation energy

Metal deformation at elevated temperature is a thermally activated process. The stress–strain behavior is described with the constitute equation:

$$\sigma = K \cdot \varepsilon^n \dot{\varepsilon}^m \cdot \exp\left(\frac{Q}{RT}\right) \quad (1)$$

where σ is the flow stress, K is a material constant, ε is the strain, $\dot{\varepsilon}$ is the strain rate, n is the stress exponent, m is the strain rate sensitivity, Q is the activation energy, R is the gas constant, and T is the absolute temperature.

When the material is superplastic, the value of n is known to be zero, and Eq. (1) can be expressed as

$$\dot{\varepsilon} = K_1 \cdot \sigma^{1/m} \cdot \exp\left(\frac{Q}{RT}\right) \quad (2)$$

According to the experimental data, the plots of $\lg\sigma$ versus $\lg\dot{\varepsilon}$ and $\lg\sigma$ versus $1/T$ are drawn as shown in Fig. 3, where the slopes of the lines can be used to measure the activation energy. The activation energy is measured as 89.4 kJ/mol, which is close to that for grain boundary diffusion (92 kJ/mol). Therefore, the dominant deformation mechanism of the alloy is most likely to be the grain boundary diffusion-controlled grain boundary slip (GBS).

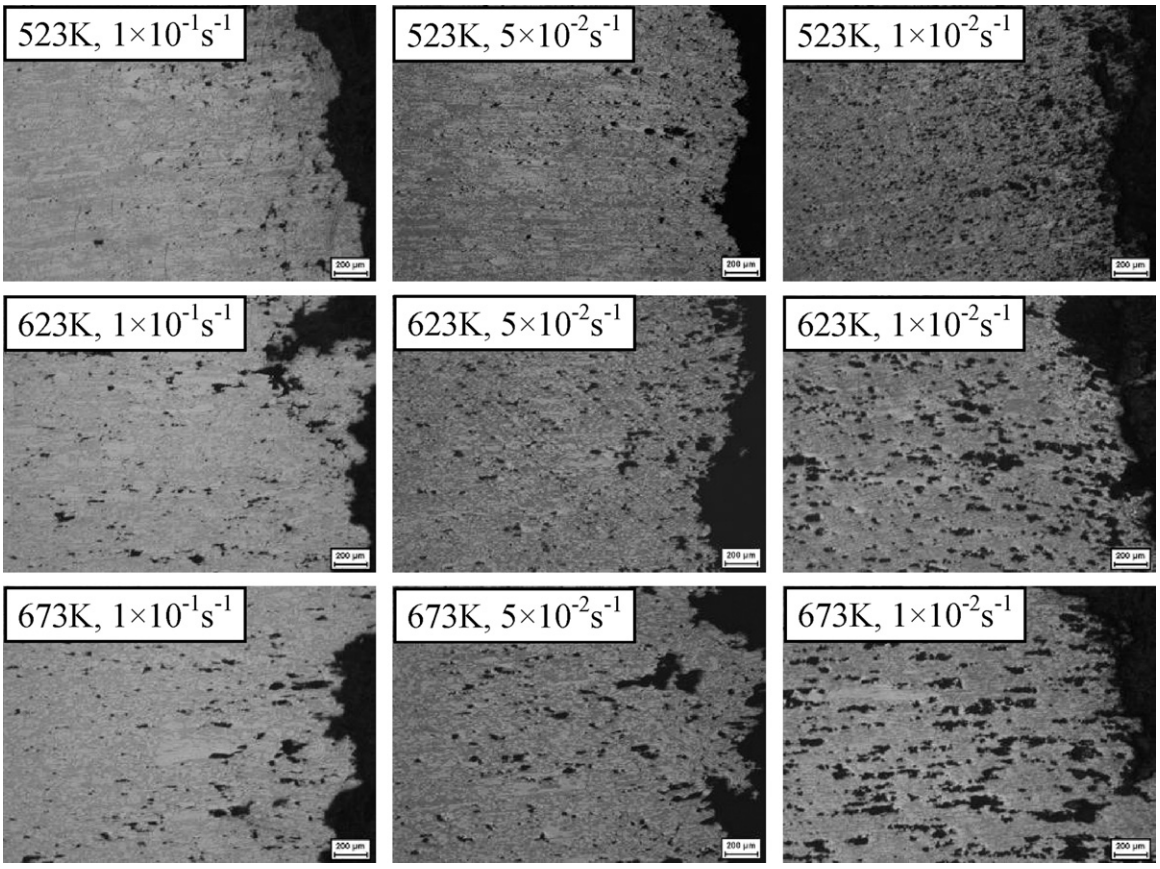

Fig. 4. Microstructures of the tensile tested specimens.

3.4. Cavitation development during the tensile testing

Cavitation is a critical feature of the failure of superplastic alloys. The cavitation development reflects the failure behavior of tensile tests [16,17]. Fig. 4 shows the cavitation distributions in the place of fracture. All specimens exhibit cavitations, and with the decrease of initial strain rate and increase of temperature, the amount and size of cavitation both increase. This demonstrates that, when the initial strain rate is relatively lower and the temperature is relatively higher, the vacancies near the grain boundaries have enough time to diffuse. The concentration of vacancies forms the cavitation, and then the cavitations concentrate and form some larger cavitations leading to the failure. These processes are all favorable for the large elongation of materials.

4. Conclusions

(1) The Mg–8Li–2Zn alloy exhibits high strain rate superplasticity with a maximum elongation of 279% at an initial strain rate of $1.0 \times 10^{-2}\ s^{-1}$ and an elongation of 151% at an initial strain rate of $1.0 \times 10^{-1}\ s^{-1}$ at 623 K.
(2) The superplastic deformation activation energy is 89.4 kJ/mol, indicating that the deformation mechanism in alloy is GBS controlled by grain-boundary diffusion.
(3) Cavities nucleate and coalesce during deformation and that is one of results leading to the fracture of the material.
(4) The amount and size of cavitation both increase with the decrease of initial strain rate or the increase of temperature.

Acknowledgements

This work was supported by the National Natural Science Foundation of China (No. 51001034) and the Fundamental Research funds for the Central Universities (HEUCF101008).

References

[1] D. Zdenek, T. Zuzanka, K. Stanislav, J. Alloys Compd. 378 (1–2) (2004) 192–195.
[2] C.L. Cui, L.B. Wu, R.Z. Wu, J.H. Zhang, M.L. Zhang, J. Alloys Compd. (2001), doi:10.1016/j.jallcom.2011.04.030.
[3] H.W. Dong, L.M. Wang, Y.M. Wu, L.M. Wang, J. Alloys Compd. 506 (1) (2010) 468–474.
[4] Z. Trojanová, Z. Drozd, P. Lukac, F. Chmelík, Mater. Sci. Eng. A 410–411 (2005) 148–151.
[5] W. Kim, M. Kim, J. Wang, Mater. Sci. Eng. A 516 (1–2) (2009) 17–22.
[6] P. Metenier, G. González-Doncel, O. Ruano, J. Wolfenstine, O.D. Sherby, Mater. Sci. Eng. A 125 (2) (1990) 195–202.
[7] O. Sivakesavam, Y.V.R.K. Prasad, Mater. Sci. Eng. A 323 (1–2) (2002) 270–277.
[8] Z.K. Qu, X.H. Liu, R.Z. Wu, M.L. Zhang, Mater. Sci. Eng. A 527 (13–14) (2010) 3284–3287.
[9] K. Higashi, J. Wolfenstine, Mater. Lett. 10 (7–8) (1991) 329–332.
[10] M. Furui, X. Cheng, T. Aida, M. Inoue, H. Anada, T.G. Langdon, Mater. Sci. Eng. A 410–411 (2005) 439–442.
[11] J. Wolfenstine, G. González-Doncel, O. Sherby, Mater. Lett. 15 (4) (1992) 305–308.
[12] Y. Yoshida, S. Kamado, Y. Kojma, Mater. Trans. 43 (10) (2002) 2419–2423.
[13] K.C. Chan, G.Q. Tong, Mater. Lett. 44 (1) (2000) 39–44.
[14] H.G. Jeong, K. Hiraga, M.S. Kim, Mater. Lett. 48 (3–4) (2001) 219–224.
[15] K.C. Chan, G.Q. Tong, Mater. Lett. 51 (5) (2001) 389–395.
[16] Y. Ma, T.G. Langdon, Acta Metall. Mater. 42 (1994) 2753–2761.
[17] M. Kawasaki, K. Kubota, K. Higashi, T.G. Langdon, Mater. Sci. Eng. A 429 (2006) 334–340.